

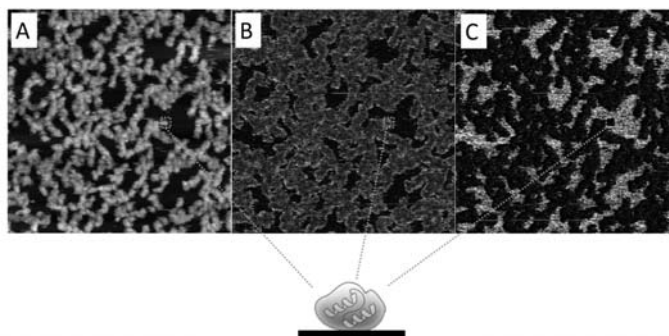
## NANOSCALE MECHANICAL PROPERTIES OF SINGLE BIOMOLECULES BY AFM

Peter SCHÖN,\* Maria GOSA and G. Julius VANCOSO

Materials Science and Technology of Polymers, MESA+ Institute for Nanotechnology, University of Twente,  
Enschede, The Netherlands

*Received December 20, 2012*

In the past 25 years the atomic force microscope (AFM) has become a true enabling platform in the life sciences opening entire novel avenues for structural and dynamic studies of biological systems. It enables visualization, probing and manipulation across the length scales, from single molecules to living cells in buffer solution under physiological conditions without the need for labeling or staining of the specimen. Currently there is a great interest in AFM based high resolution mechanical mapping techniques providing single molecule resolution of mechanical properties to derive molecular structure-function relationships. In this article selected examples of the recent literature are highlighted including own results obtained by peak force tapping AFM to elaborate the mechanical properties of lysozyme molecules adsorbed to mica substrates.



### INTRODUCTION

Since its invention in 1986<sup>1</sup> the atomic force microscope (AFM) has evolved from a high resolution imaging microscopy technique into a true enabling platform in the life sciences. Importantly, biological systems can be studied under physiological conditions without the need for labeling or staining of the samples which makes the AFM a unique high resolution imaging instrument. Due to its force sensing capabilities it opened entirely novel avenues to study the correlation of reactivity with mechanical properties and elucidate structure-function relationships of single biomolecules under physiological relevant conditions in buffer solution.<sup>2-6</sup>

Quantitative mechanical information on biological samples has been obtained by nanoindentation<sup>7</sup> and force volume imaging.<sup>8</sup> Using appropriate mechanical contact models, local elastic moduli can be derived from the recorded force vs. deformation curves. Serious drawbacks for nanoindentation and force volume imaging are the poor lateral resolution and the extensive time required to obtain a complete mapping of the surface.

In recent years there has grown a great interest to obtain mechanical property maps in concert with the correlated topography at nanoscale resolution at typical AFM imaging speeds. Despite the tremendous progress in AFM technology development this has remained a notoriously

\* Corresponding author: p.m.schon@utwente.nl; +31-53-4893170 (office); +31 (0)53 489 3823 (fax)

difficult task to obtain quantitative mechanical maps of biological systems, like lipid bilayers or protein membranes with high resolution. Tapping mode imaging was a pivotal development in AFM technology and became a routinely used imaging mode to study biological specimen, allowing gentle scanning with significantly reduced lateral forces. However, it does not provide quantitative mechanical maps because the phase signal is related to the energy dissipation of the tapping tip. There is an ongoing effort in academic research and industrial instrumental development aiming at improved or fundamentally new imaging modes enabling quantitative high resolution mechanical imaging by AFM. In general, three main evolving technological approaches can be distinguished, including multifrequency tapping<sup>9</sup>, pulsed force techniques<sup>9-11</sup> and contact resonance techniques<sup>12</sup> which operate in contact mode with dynamic excitation at or near the cantilever resonance. In addition to sample topography, these multi parameter force mapping approaches simultaneously

provide mechanical parameters such as stiffness, adhesion and energy dissipation. To date the different technical approaches are being continuously developed and commercialization is also underway by different manufactures.

Fundamental breakthroughs in biological AFM based mechanical property mapping have been achieved recently. Real-time simultaneous topographic and mechanical mapping with high spatial resolutions down to the molecular level have been demonstrated on short DNA nucleotides and various membrane proteins in buffered liquid environment using torsional harmonics cantilever introduced from Sahin and co-workers.<sup>13</sup> Strikingly, the hybridization of surface attached ssDNA to a complementary ssRNA could be detected by a significantly decreased stiffness of the dsDNA/RNA hybrid compared to the ssRNA (Fig. 1). These findings might lead to completely novel assays with nanomechanical, label free read out and dramatically increased sensitivity, being in the attomolar regime.

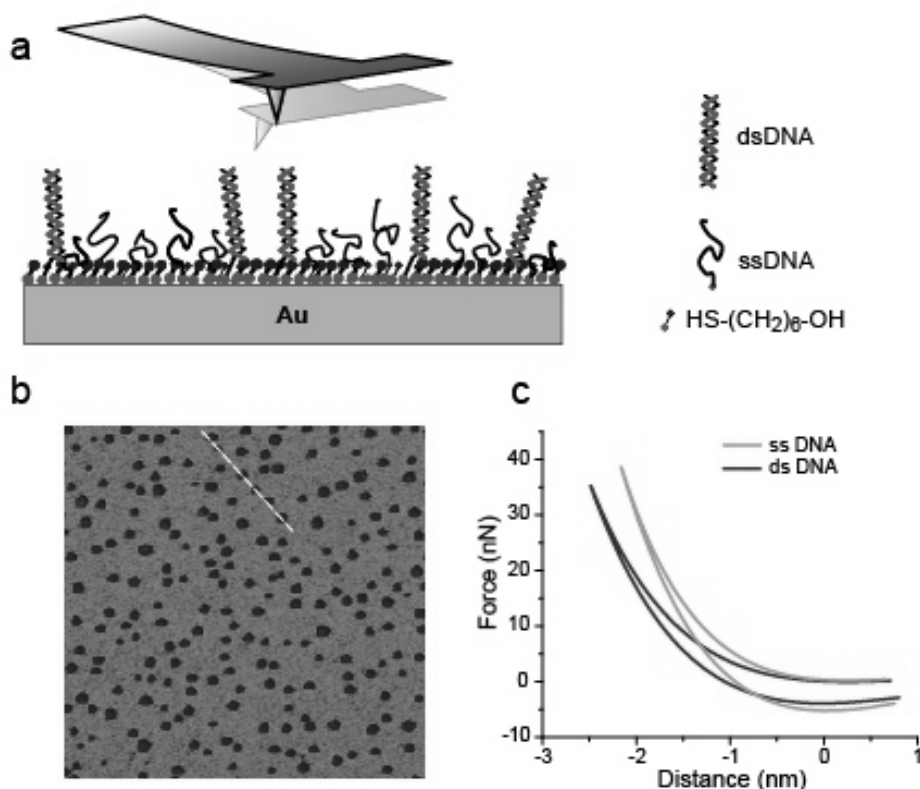


Fig. 1 – Nanomechanical detection of DNA hybridization. (a) Schematic of the experiment. After hybridization, the surface of the array spot is scanned with the AFM to generate the stiffness map shown in (b). Scan size is 3  $\mu\text{m}$ . Hybridized molecules are measured to be less stiff and appear as dark brown spots. (c) Stiffness at each pixel in (b) is calculated from force-distance curves [with permission, adapted from reference 13].

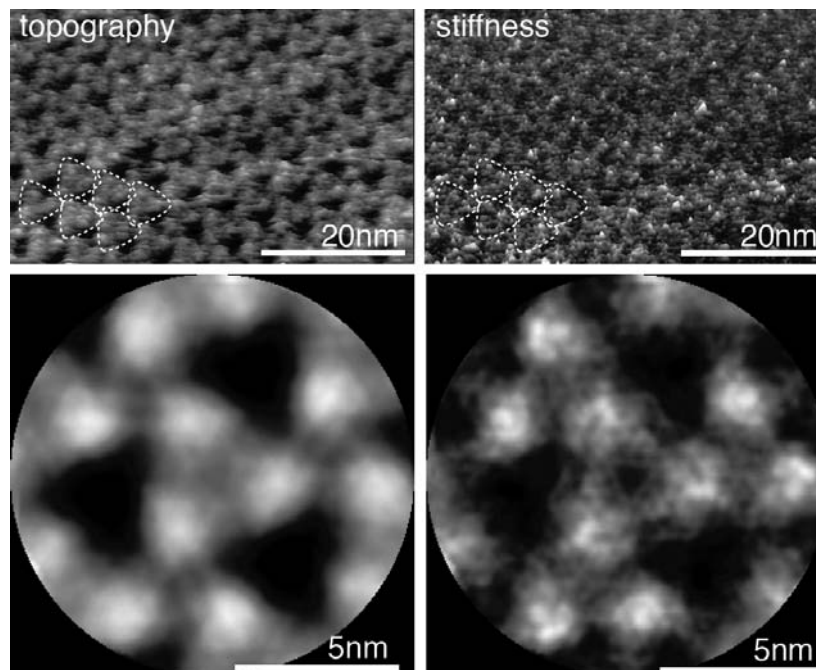


Fig. 2 – High-resolution images of topography and stiffness of bacteriorhodopsin molecules. Individual trimers are encircled. 3-fold symmetrized correlation average topograph (C) and stiffness (D) calculated from 13 bacteriorhodopsin trimers from A and B and overlaid with the atomic structure. Individual loops are labeled [with permission, adapted from reference 18].

Importantly, this demonstrates impressively the intimate coupling of chemical and mechanical information at the molecular scale. Garcia and co-workers introduced bimodal excitation and frequency modulation force microscopy.<sup>9</sup> They report from the mapping of the protein structural flexibility with sub-2-nm spatial resolution in liquid.<sup>14</sup> This was achieved by excitation of two cantilever eigenmodes in dynamic force microscopy enabling the separation between topography and flexibility mapping. It was possible to measure variations of the elastic modulus in a single antibody pentamer along the protein structure from the end of the protein arm to the central protrusion. In focus of recent AFM based nanoscale mechanical mapping studies was the membrane protein bacteriorhodopsin.<sup>15-17</sup> With mechanical mapping nanoscale information can be obtained that allows assigning protein domains to their mechanical function, for example thereby explaining its physiological function as proton pump. It was possible to correlate protein flexibility with crystal structure utilizing high resolution mechanical mapping providing submolecular resolution (Fig. 2).

In particular, it was concluded that R-helices are stiff structures that may contribute importantly to the mechanical stability of membrane proteins, while interhelical loops appeared more flexible, allowing conformational changes related to function.<sup>18</sup>

Extensive research has been done from different groups on amyloid fibrils to quantify their

nanomechanical properties.<sup>19,20</sup> Very recent reports on nanomechanical properties cover a wide range of further biological systems including lipid bilayers,<sup>21</sup> erythrocyte membranes,<sup>22</sup> living cells<sup>20</sup> and marine diatoms,<sup>23</sup> Finally, the AFM based nanomechanical mapping techniques were used for adhesion mapping to detect biomolecular interaction of avidin-biotin<sup>24</sup> and high-resolution imaging of chemical and biological sites on living yeast cells,<sup>25</sup> For these experiments chemically modified AFM tips were used to maintain chemical and biological specific probing of adhesion forces.

In the work presented here peak force tapping AFM was utilized to elaborate the nanoscale mechanical properties of lysozyme molecules adsorbed to mica substrates.

Peak force tapping AFM has been introduced as an AFM based mechanical property mapping technique. In a peak force tapping experiment the sample is oscillated at a rate well below the resonance frequency of the AFM cantilever. The AFM feedback uses the maximum force load (peak force) as its control signal to maintain a constant imaging force. As a result multiple force vs. time curves are being recorded and averaged on each probed sample pixel. From the corresponding force distance curves mechanical parameters like adhesion, deformation and the elastic modulus are determined as illustrated in Fig. 3.

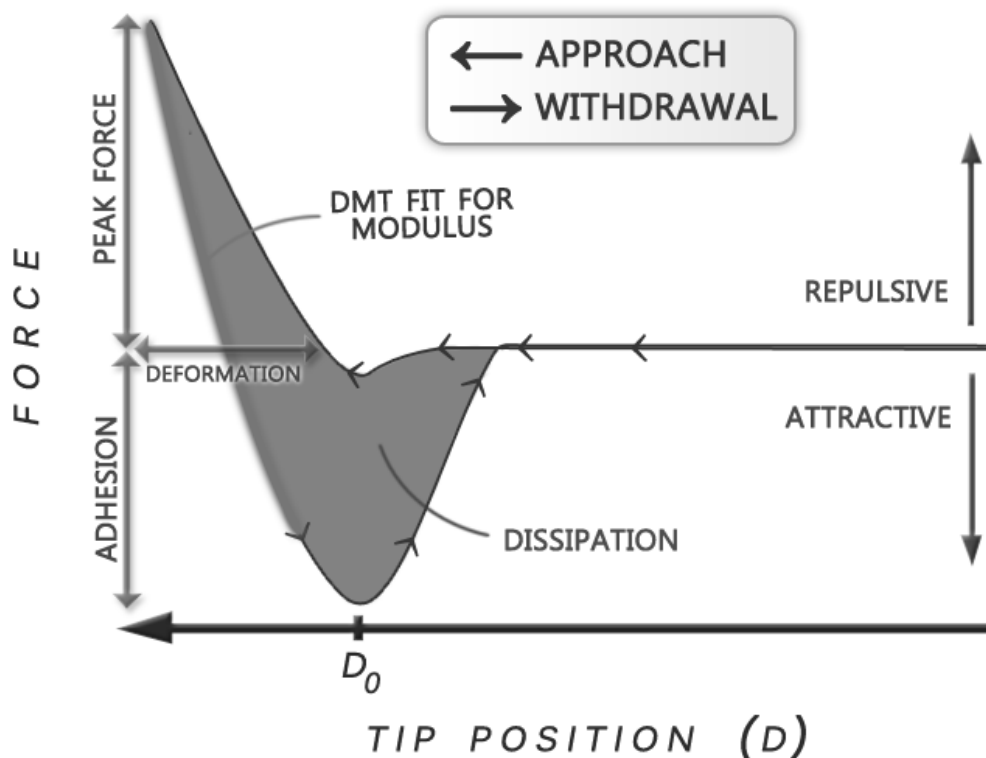


Fig. 3 – Schematic force distance curve derived during mechanical mapping with peak force tapping AFM with derivation of different mechanical parameters.

In order to estimate the elastic modulus from the force distance curves the Derjaguin–Müller–Toporov (DMT) mechanical contact model was used in our experiments. According to the DMT model the forces of the AFM tip-surface interaction are:

$$F_{interaction} = \frac{4}{3}E^* \sqrt{r(d-d_0)^3} + F_{adh}$$

where  $F_{interaction}$  is the tip-sample-force,  $E^*$  is the reduced elastic modulus,  $r$  is the contact radius of the AFM tip,  $d_0$  is the surface rest position,  $(d-d_0)$  is the deformation of the sample and  $F_{adh}$  is the adhesion force. The DMT model was found to be useful for samples with moderate adhesion levels and AFM tips with small radii. Importantly, it allows feasible computation, rendering it favorable for real time imaging. It is important to mention that independently of the chosen contact mechanical model the AFM tip geometry, its penetration depth and hence the contact area as expressed in the contact radius  $r$  do have a pronounced effect on the values of the moduli obtained. This is corrected to some extent by using a calibration procedure with an appropriate polymeric sample of known modulus. In the measurements the same setpoint is chosen as for

the calibration.<sup>26</sup> Still local topography or roughness can have an impact on the measured moduli values due to variation in contact radii. Consequently flat samples with minimal roughness represent optimal specimen for the AFM based mechanical mapping procedures.

## EXPERIMENTAL

### Sample preparation

Lysozyme from chicken egg white (CAS no. 12650-88-3, dialyzed, lyophilized, powder), was purchased from Sigma-Aldrich (St. Louis, MO, USA) and used without further purification. All solvents were of high purity, and deionized water from a Milli-Q water purification system was used throughout. The following buffers were used for AFM imaging and/or sample preparation: a) 5 mM  $\text{KH}_2\text{PO}_4$ , pH 6; b) 10 mM Tris-HCl, 150 mM KCl, pH 7.4; c) phosphate buffered saline (PBS) (pH 7.4, 150 mM NaCl) was used as received (B. Braun Melsungen AG, Melsungen, Germany). Mica discs were glued to steel discs with cyanuracrylate and left in air for overnight. The mica was cleaved with tape immediately before use. Chicken egg white lysozyme was adsorbed on the freshly cleaved mica. For this purpose a solution of lysozyme (1  $\mu\text{g}/\text{ml}$ ) in phosphate buffer containing 5 mM  $\text{KH}_2\text{PO}_4$  at pH 6 was incubated for 20 minutes. The enzyme solutions were prepared freshly from the lyophilized powder before each experiment. After incubation the solution was exchanged against the same potassium phosphate buffer without enzymes. To obtain a monolayer of lysozyme on the

mica surface, a 10 fold higher concentration of lysozyme was used (0.1 mg/mL in 5 mM  $\text{KH}_2\text{PO}_4$  at pH 6).

#### AFM measurements

A Multimode 8 AFM instrument equipped with a NanoScope V controller and NanoScope version 8.10 software (Bruker Nano, Santa Barbara, CA) was used. Peak Force Tapping was done with Si tips on SiN cantilevers (SCANASYST-Fluid<sup>+</sup>, Bruker AFM Probes, Camarillo, CA) in liquid buffered environment. Cantilever spring constants were determined using the thermal tune method<sup>27</sup> and showed values in the range of  $\sim 0.5$  N/m. PF-QNM AFM was done at a constant oscillation of the sample at 2 kHz using amplitudes of 30-120 nm and peak forces of 100-850 pN. Scanning was performed at a speed of 1-2 lines/s. Image processing and data analysis were performed with the NanoScope software version 8.10, and NanoScope Analysis software version 1.10.

## RESULTS AND DISCUSSION

Here we describe the mechanical properties of surface adsorbed lysozyme. Lysozyme is a globular protein with a molecular mass of 14.4 kDa. It damages bacterial cell walls by hydrolyzing  $\beta(1\rightarrow4)$  glucosidic bonds in the peptidoglycan layer of bacteria. In our studies the enzyme was adsorbed from solution to a freshly cleaved mica surface due to electrostatic interaction. Mechanical maps of lysozyme monolayers were obtained in physiological buffered environment, both on (diluted) monolayers as well as single enzymes providing DMT modulus and deformation maps (Fig. 4). The study of mechanical properties of proteins such as deformability and flexibility is of

fundamental importance since protein functions and their three-dimensional conformations are intimately connected. A few cases are reported in the literature where AFM has been used to compress protein molecules to extract information on the apparent Young's moduli of single molecules or monolayers.<sup>28</sup> Strikingly, the denaturation process of a single protein could be detected in this manner.<sup>29</sup>

Adhesion differences were minimal (data not shown). The height values varied between  $\sim 2$ -3 nm and lateral dimensions were also in excellent agreement with the molecular dimensions. Deformations were recorded between 0.5-1 nm which indicates a partial compression of the molecules, assuring to not completely compress the molecule and thereby minimize also the influence of the underlying substrate. On the other hand, the molecule must be compressed to some extent to be able to determine elastic moduli. DMT modulus values obtained on the lysozyme samples showed mean values of  $\sim 140$ -200 MPa with an entire modulus value range from  $\sim 80$ -250 MPa. We found good agreement with literature values obtained by AFM force volume (FV) imaging in previous studies of  $500 \pm 200$  MPa obtained on lysozyme<sup>28</sup> and  $600 \pm 200$  MPa on lactate oxidase.<sup>30</sup> This elasticity is also in good agreement with values obtained by measuring the macroscopic compressibility of wet lysozyme crystals (0.2-1 GPa).

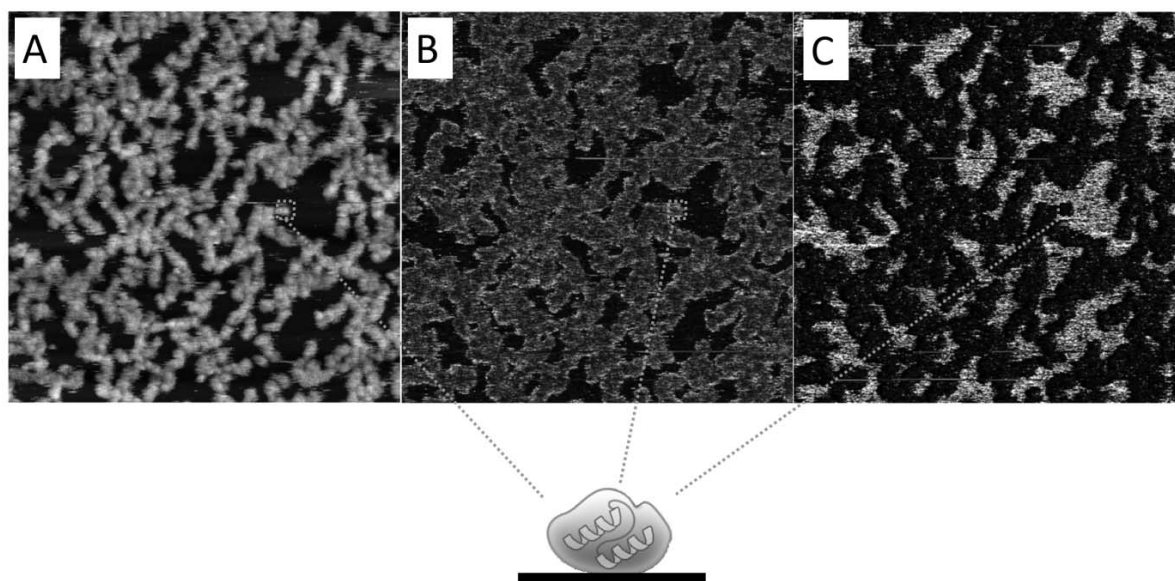


Fig. 4 – Lysozyme molecules adsorbed to mica at submonolayer coverage, imaged by peak force tapping AFM in physiological buffer. For illustration a single enzyme is localized in the different data channels obtained simultaneously in one scan; corresponding measures on the lysozyme layer in brackets. (A): height (z-scale: 5 nm); (B): deformation (z-scale: 1.8 nm); (C): DMT modulus (z-scale: 1 GPa); scan size: 250x250 nm.

However these modulus values are at least 1-2 orders of magnitude larger than the ones recorded on the native purple membrane (PM) from *Halobacterium salinarum*<sup>16</sup> which consists of the light-driven proton-pump bacteriorhodopsin (BR) and lipids. The Young's moduli of both PM surfaces revealed  $10 \pm 5$  MPa in one study.<sup>16</sup> These significantly lower modulus values may be due to the presence of the lipids which are softer than the protein and the 2D nature of the membrane. Lateral mobility within the membrane might lead to an apparent softening of the sample under gentle indentation forces. The possible contribution of an underlying hard substrate on the elastic properties of thin enzyme layers must be carefully elaborated and is currently under investigation, in addition to probing frequency dependencies. In this regard similar mechanical performance was found for bacteriorhodopsin at 2 kHz<sup>18</sup> and  $\sim 50$  kHz<sup>17</sup> probing frequencies.

It was reported that the hard underlying mica substrate did not affect significantly the determination of the mechanical properties for a 2.8 nm thick lipid bilayer film at the applied forces (ca. 250 pN)<sup>40</sup>. Previously the contribution of a hard substrate on the determination of the elastic properties of thin layers has been shown to be <25% for deformations of ca. 20% of the layer thickness. Hence we assume that in our case the influence of the underlying substrate was minimal as we applied forces of ca. 220 pN.

The used AFM tips had very small nominal radii of 2–3 nm. Thus we assume that local averaging at boundaries is minimal. Moreover, these small tip radii in combination with the ultraflat mica substrate also minimize potential modulus errors. Significant tapping frequency dependencies were reported recently in lower frequency regimes (<  $\sim 600$  Hz) on low density polyethylene (LDPE) with comparable bulk elastic moduli<sup>31</sup>. For the lysozyme samples no substantial frequency dependences are anticipated in the applied tapping frequency (2 kHz). For a polymeric sample we found similar modulus values at 2 kHz and higher probing frequencies ( $\sim 50$  kHz) utilizing a multifrequency approach.<sup>26</sup>

## CONCLUSIONS

AFM has evolved from a high resolution imaging tool into a mechanical mapping technique providing topography and quantitative mechanical

maps simultaneously. There is a great interest in AFM based high resolution mechanical mapping techniques providing single molecule resolution of mechanical properties to derive molecular structure-function relationships. The feasibility of peak force tapping AFM to obtain mechanical maps on lysozyme monolayers on mica has been demonstrated in this article. Despite the remarkable progress in the development of the AFM based mechanical imaging technology including commercial availability, a number of physical aspects must be addressed in the future and taken into careful consideration: effects of surface roughness and frequency of probing, the potential impact of the underlying hard substrate if molecular films or biomolecules are investigated.

*Acknowledgements:* P.S., M.G. and G.J.V. thank the MESA+ Institute for Nanotechnology for funding. P.S. acknowledges the COST Action TD1002: 'European network on applications of Atomic Force Microscopy to NanoMedicine and Life Sciences' for providing fruitful discussions and collaborations.

## REFERENCES

1. G. Binnig, C.F. Quate and C. Gerber, *Physica Review Letters*, **1986**, *56*, 930-933.
2. H. Gump, E.M. Puchner, J.L. Zimmermann, U. Gerland, H.E. Gaub and K. Blank, *Nano Letters*, **2009**, *9*, 3290-3295.
3. S. Zou, M.A. Hempenius, H. Schönherr and G.J. Vancso, *Macromolecular Rapid Communications*, **2006**, *27*, 103-108.
4. T. Hügél, N.B. Holland, A. Cattani, L. Moroder, M. Seitz and H.E. Gaub, *Science*, **2002**, *296*, 1103-1106.
5. W.Q. Shi, M.I. Giannotti, X. Zhang, M.A. Hempenius, H. Schönherr and G.J. Vancso, *Angewandte Chemie International Edition*, **2007**, *46*, 8400-8404.
6. C. Schäfer, R. Eckel, R. Ros, J. Mattay and D. Anselmetti, *J. of the American Chem. Soc.*, **2007**, *129*, 1488-1489.
7. M. Stolz, R. Gottardi, R. Raiteri, S. Miot, I. Martin, R. Imer, U. Staufer, A. Raducanu, M. Duggelin, W. Baschong, A.U. Daniels, N.F. Friederich, A. Aszodi and U. Aebi, *Nature Nanotechnology*, **2009**, *4*, 186-192.
8. W.F. Heinz and J.H. Hoh, *Trends in Biotechnology*, **1999**, *17*, 143-150.
9. R. Garcia and E.T. Herruzo, *Nature Nanotechnology*, **2012**, *7*, 217-226.
10. H.U. Krottil, T. Stifter, H. Waschipky, K. Weishaupt, S. Hild and O. Marti, *Surface and Interface Analysis*, **1999**, *27*, 336-340.
11. O. Sahin, S. Magonov, C. Su, C.F. Quate and O. Solgaard, *Nature Nanotechnology*, **2007**, *2*, 507-514.
12. K. Wadu-Mesthrige, N.A. Amro, J.C. Garmo, S. Cruchon-Dupeyrat and G.Y. Liu, *Applied Surface Science*, **2001**, *175*, 391-398.
13. S. Husale, H.H.J. Persson and O. Sahin, *Nature*, **2009**, *462*, 1075-1078.

14. D. Martinez-Martin, E.T. Herruzo, C. Dietz, J. Gomez-Herrero and R. Garcia, *Physical Review Letters*, **2011**, *106*, 198101-198104.
15. F. Rico, C. Su and S. Scheuring, *Nano Letters*, **2011**, *11*, 3983-3986.
16. I. Medalsy, U. Hensen and D.J. Müller, *Angewandte Chemie International Edition*, **2011**, *50*, 12103-12108.
17. M.D. Dong, S. Husale and O. Sahin, *Nature Nanotechnology*, **2009**, *4*, 514-517.
18. F. Rico, C.M. Su and S. Scheuring, *Nano Letters*, **2011**, *11*, 3983-3986.
19. K. Sweers, K. van der Werf, M. Bennink and V. Subramaniam, *Nanoscale Research Letters*, **2011**, *6*, 1-10.
20. J. Adamcik, A. Berquand and R. Mezzenga, *Applied Physics Letters*, **2011**, *98*, 193701-193703.
21. L. Picas, F. Rico and S. Scheuring, *Biophysical Journal*, **2012**, *102*, L01-L03.
22. L. Picas, F. Rico, M. Deforet and S. Scheuring, *ACS Nano*, **2013**, *7*, 1054-1063.
23. G. Pletikapic, A. Berquand, T.M. Radic and V. Svetlicic, *Journal of Phycology*, **2012**, *48*, 174-185.
24. M. Dong and O. Sahin, *Nat. Commun.*, **2011**, *2*, 247.
25. D. Alsteens, V. Dupres, S. Yunus, J.P. Latge, J.J. Heinisch, Y.F. Dufrene, *Langmuir*, **2012**, *28*, 16738-16744.
26. P. Schön, K. Bagdi, K. Molnar, P. Markus, B. Pukanszky and G.J. Vancso, *European Polymer Journal*, **2011**, *47*, 692-698.
27. J.L. Hutter and J. Bechhoefer, *Review of Scientific Instruments*, **1993**, *64*, 1868-1873.
28. M. Radmacher, M. Fritz, J.P. Cleveland, D.A. Walters and P.K. Hansma, *Langmuir*, **1994**, *10*, 3809-3814.
29. R. Afrin, M.T. Alam and A. Ikai, *Protein Science*, **2005**, *14*, 1447-1457.
30. A. Parra, E. Casero, E. Lorenzo, F. Pariente and L. Vazquez, *Langmuir*, **2007**, *23*, 2747-2754.
31. K.K.M. Sweers, K.O. van der Werf, M.L. Bennink and V. Subramaniam, *Nanoscale*, **2012**, *4*, 2072-2077.

